



Hydrogeology and geochemistry of near-shore submarine groundwater discharge at Flamengo Bay, Ubatuba, Brazil

June A. Oberdorfer ^{a,*}, Matthew Charette ^b, Matthew Allen ^b,
Jonathan B. Martin ^c, Jaye E. Cable ^d

^a Department of Geology, San Jose State University, One Washington Square, San José, CA 95192-0102, USA

^b Woods Hole Oceanographic Institution, USA

^c University of Florida, USA

^d Louisiana State University, USA

Received 14 September 2006; accepted 21 July 2007

Abstract

Near-shore discharge of fresh groundwater from the fractured granitic rock at Flamengo Bay, Ubatuba, Brazil, is strongly controlled by the local geology. Freshwater flows primarily through a zone of weathered granite to a distance of 24 m offshore. In the nearshore environment this weathered granite is covered by about 0.5 m of well-sorted, coarse sands containing pore water with sea water salinity, with an abrupt transition to much lower salinity once the weathered granite is penetrated. Further offshore, low-permeability marine sediments contain saline porewater, marking the limit of offshore migration of freshwater. Freshwater flux rates based on tidal signal and hydraulic gradient analysis indicate a fresh submarine groundwater discharge of 0.17–1.6 m³/day per m of shoreline. Dissolved inorganic nitrogen and silicate are elevated in the porewater relative to seawater, and appeared to be a net source of nutrients to the overlying water column. The major ion concentrations suggest that the freshwater within the aquifer has a short residence time. Major element concentrations do not reflect in situ alteration of the granitic rocks, possibly because the alteration occurred prior to development of the current discharge zones, or because of large volumes of water discharge in this high rainfall region.

© 2007 Published by Elsevier Ltd.

Keywords: submarine groundwater discharge; porewater geochemistry; nutrient fluxes

1. Introduction

While there has been growing interest over the last two decades in quantifying the discharge of groundwater to the coastal zone, the majority of studies have been carried out in aquifers consisting of unlithified sediments or in karst environments. This study is part of an intercomparison experiment that examines a range of techniques used to quantify submarine groundwater discharge (SGD) in a fractured-rock aquifer environment. This is a difficult environment to evaluate due to the spatial variability in aquifer properties resulting from the

variability in the spacing, aperture, and interconnectedness of the fractures. While the intercomparison experiment examines SGD on a variety of scales, the work reported on here quantifies SGD on the small scale of a beach transect in the near-shore region where much of the discharge is expected to take place. Previous SGD studies (for example, Harvey and Odum, 1990; Vanek, 1993; Nuttle and Harvey, 1995; Staver and Brinsfield, 1996; Robinson, 1996) have been carried out on a small scale (tens to hundreds of meters), while previous SGD intercomparison experiments (Burnett et al., 2002; Burnett et al., 2006; Martin et al., 2007) have examined SGD on multiple scales, including the local scale.

The granitic rocks of the study area are representative of the extensive Pre-Cambrian shield region of eastern Brazil.

* Corresponding author.

E-mail address: june@geosun.sjsu.edu (J.A. Oberdorfer).

Groundwater occurs in fractures in the granitic and metamorphic rocks of the area. Not a great deal is known about the groundwater in the fractured bedrock since it is not used to a significant degree as a resource. There is some utilization of localized springs related to major fractures. The region is one of the highest rainfall (2000–4000 mm/year) regions of Brazil (Rebouças, 2002) which means recharge is likely to occur readily. Rainfall was relatively light (13 mm in 7 days, based on local weather station data) during the period of this study which was conducted towards the beginning of the rainy season. SGD would most likely be greater towards the end of the rainy season.

Understanding SGD on this small scale should provide insight into scaling effects when compared to data collected on the much larger scale of some of the geochemical tracer studies (Burnett et al., 2006; this issue) that were being carried out at the same time. This study also documents groundwater discharge in a geologic environment that was poorly documented previously. The location of the field area is given in Fig. 1. Enseada de Flamengo (Flamengo Bay), near Ubatuba, São Paulo state, is the location of the marine laboratory of the University of São Paulo. The beach at the marine laboratory was selected for in-depth studies because of the presence of weathered bedrock and sediment above the fractured granite; this granular material permitted the installation of wells and equipment that would not have been possible to install in fresh, fractured bedrock.

2. Methods

2.1. Piezometer installation

Within this nearshore beach site, wells were installed in two stages. Nine small-diameter (5 cm), shallow wells were installed by a Brazilian consulting company (Gea) in October 2001. In November 2003, during our intercomparison experiment, eight temporary piezometers were installed for the purpose of collecting pore waters for (bio)geochemical analysis: four multi-level piezometers capable of providing access to discrete pore water depths down to 2.3 m (MS-2, -3, -4, -5) and two very small diameter (1-cm) vapor-probe wells (WH-1, -2). These wells are described in more detail in Section 2.7.

Wells installed in 2001 are labeled well 0, A1, A2, A3, B1, B2, B3. Two of the wells installed in the inter-tidal zone were subsequently destroyed prior to the start of the 2003 intercomparison experiment. The locations of the remaining seven wells are shown in Fig. 2. Well 0 was completed at a depth of 5.0 m below ground surface (bgs), while the depth of completion of the remaining wells ranged from 0.7 to 2.1 m bgs. During the installation of well 0, 3 m of saturated, weathered granite were encountered; most of the groundwater is expected to flow through this sandy, decomposed granite since it is expected to be more permeable than the underlying fresher granite. These wells were hand-augered and completed with perforated PVC pipe with plastic screen clamped around the perforated section to minimize seepage of sediment into the wells. During installation of the onshore wells (wells 0, A1 and B1), augering had to

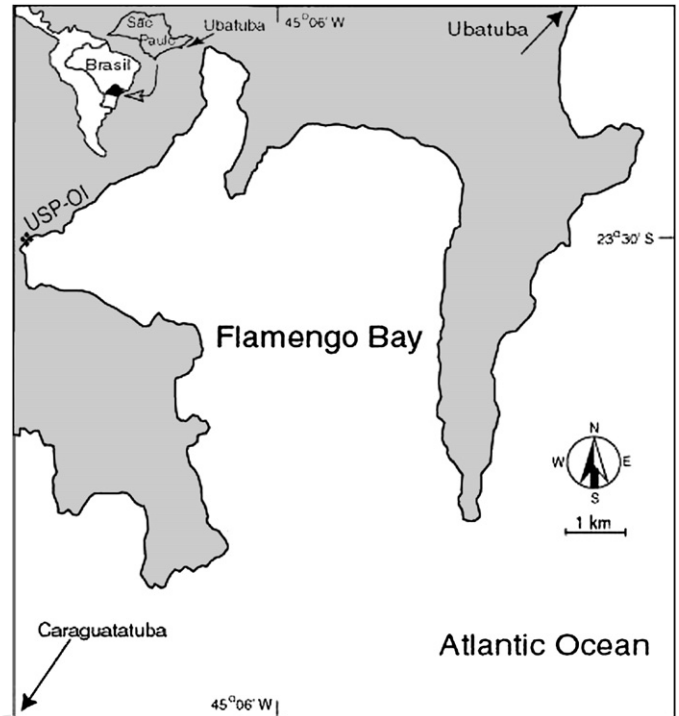


Fig. 1. Map showing location of field site at the University of São Paulo Oceanographic Institute (USP-OI).

stop when geologic materials too hard to auger through by hand were encountered. For the wells completed offshore, all well-casings extended well above the high tide level.

2.2. Coring

Sediment cores were collected near the two vapor-probe wells (WH1 and WH2; see Fig. 2 for locations relative to other

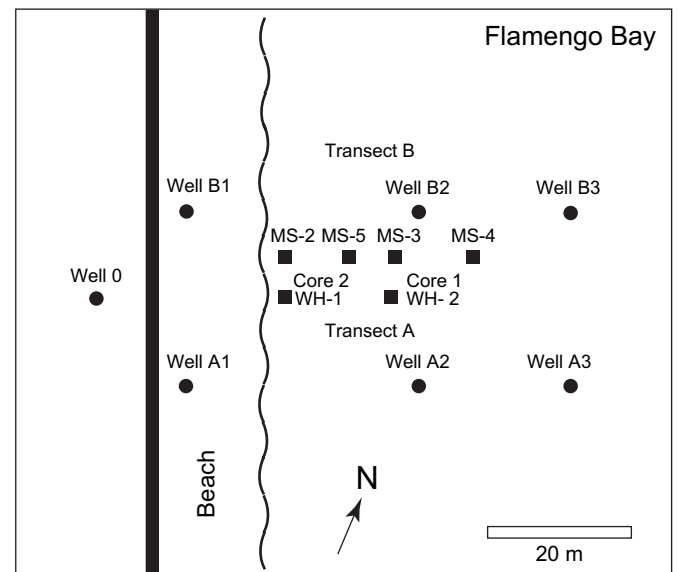


Fig. 2. Location map for field installations (Transect A with A-wells, Transect B with B-wells, piezometer and coring sites) at USP-OI at Flamengo Bay.

wells). Ten centimeter diameter aluminum irrigation tubing was driven into the sediment using a slide hammer and recovered with a makeshift tripod and come-along. Core 1 (located at well WH2) was approximately 190 cm long and core 2 (well WH1) was 100 cm. The cores were extruded onto plastic sheeting and the sediment characteristics were logged in ~13 cm intervals.

2.3. Water level measurements

Water levels in the wells were measured manually with an electric well sounder. Water levels were measured and recorded at well 0 and a stilling well on the adjacent marine laboratory dock using an ultrasonic electronic water level data logger (Infinities USA Inc.).

2.4. Slug/bail tests

Slug/bail tests were performed by either bailing (wells 0 and B1) or pumping (wells A2, A3, B2, B3) the well to lower the water level followed by monitoring of the water level recovery. This rapid change in water level in the well induces flow from the aquifer, and the rate of water level recovery is proportional to the permeability of the geologic materials. In the case of the two bailed wells, the bailed water was later reintroduced into the well to cause a water level rise, and the recovery to the original level was monitored. Offshore wells (A2, A3, B2, B3) were pumped using a GeoTech peristaltic pump. In all cases, water levels were recorded manually and replicate field tests (two to four) were performed whenever possible on each well. The data from the slug/bail tests was analyzed using the method of Hvorslev (1951) to obtain effective hydraulic conductivity of the sediments surrounding these wells.

2.5. Tidal signal analysis

Bay and well 0 water level data were collected for approximately 1 week. These data were analyzed for tidal lag (time between maximum or minimum water levels in the ocean and corresponding maximum or minimum water levels in the well) and tidal efficiency (ratio of water level change in the well to that in the ocean over a half tidal cycle). The rate (tidal lag) and magnitude (tidal efficiency) with which the tidal signal propagates into the aquifer is a function of the permeability and fluid storage properties of the aquifer. The tidal lag and efficiency were used to calculate the hydraulic conductivity of the aquifer using the method of Jacob (1950).

2.6. Mini-wellpoint sampling for salinity

Small diameter (1 cm) metal wellpoints, perforated over a 2 cm interval near the pointed tip, were hand pushed into the sediment to depths of up to 1 m. Porewater was sampled by purging the wellpoint of 250 ml of water, followed by collecting of a 100 ml water sample. The salinity of each water sample was read on a refractometer.

2.7. Water quality sampling and analysis

Porewater from the two vapor-probe wells (WH1 and WH2) was collected using a direct-push, shielded-screen piezometer (AMS, Inc. Madison, Wisconsin USA). Samples were collected at 15 or 30 cm intervals using a peristaltic pump coupled with Teflon tubing. At each interval, salinity and other ancillary water quality properties were measured with a YSI 600R multi-probe mounted in a flow-through cell. After several volumes of the tubing were flushed, filtered samples for nutrient determination were collected and stored frozen until analysis. Back in the laboratory, nutrient samples were thawed and run on a Lachat QuickChem 8000 flow injection analyzer using standard colorimetric techniques.

Four multisamplers (multi-level piezometers; Martin et al., 2003) were installed in a transect extending approximately 35 m offshore. The multisampler closest to shore (MS-2) was located 2.5 m from the low tide line, and the remaining three multisamplers MS-5, MS-3, and MS-4 were installed at distances of 6.5, 10.5 and 35 m from the low tide line. All multisamplers were installed to depths of 230 cm below the seafloor, but only the two farthest offshore yielded water from all eight ports; water could not be pumped from the lowest three ports of MS-2 and the lowest two ports from MS-5. One multisampler per day was sampled between November 16 and November 20, 2003. Water was initially pumped from MS-3 on November 17, 2003, and then again on November 18, 2003, as a comparison with the previous sampling time. No samples were collected when it was pumped the second time, but field parameters (salinity, DO, and pH) were measured in situ. When values of these field parameters were stable, water samples were collected in 30 ml Nalgene HDPE bottles. Two bottles were collected, one was filtered and acidified, and the other was collected as a raw sample. Chloride concentrations of the water was measured by titration with AgNO_3 . Sodium and potassium concentrations were measured with ion chromatography.

3. Results

3.1. Hydrogeologic conceptual model

The hydrogeology in the immediate vicinity of the marine laboratory was studied using geologic descriptions made during the installation of the nine wells at the site, through excavations along the beach, via cores sampled in the area of the two transects, and during installation of pore water samplers offshore. Onshore, the geologic materials consisted of about 3 m of colluvial material overlying highly weathered, granitic bedrock (to the total depth of the boring for well 0 at 5 m). Along the beach (wells A1 and B1 and the two destroyed wells, located near the low tide line) about 1 m of sand was found to overlie granitic boulders that made well installation difficult. In the nearshore submerged region, deposits consisted of about 0.5 m of coarse sand overlying about 0.3 m of hard sand with gravel, organics, and fines (Fig. 3) sitting atop highly weathered bedrock. About 24 m offshore there



Fig. 3. Photograph of core sample showing transition from overlying sand to hard layer atop the weathered bedrock.

was a fairly abrupt transition to fine marine sediment over 2 m thick. A hydrogeologic cross-section is given in Fig. 4.

Sediment cores recovered revealed a thin layer (~ 0.5 – 2 m) of sediment on top of deeply weathered crystalline bedrock. Most of the sediments, excluding the nearshore surface samples, were very poorly sorted. From the two recovered cores, most intervals contained a small amount of sand, silt, clay, and shell hash. In the offshore core (core 1) the silts and clays throughout were low permeability making this location a poor conduit for SGD. In the nearshore core 2, the surficial sediments were extremely coarse grained and had been well sorted, presumably by wave action. The transition from well-sorted coarse sands to poorly sorted sands, silts and clays is shown in Fig. 3.

3.2. Slug testing

Slug tests were performed on well 0, completed in the weathered bedrock, and well B1, completed in sand among boulders. The results for the slug and bail tests on well 0 gave an average hydraulic conductivity for the weathered granitic bedrock of 1.0×10^{-4} cm/s (0.09 m/day). The results for the slug and bail tests on well B1 yielded an average hydraulic conductivity for the sandy beach material of 2.9×10^{-3} cm/s (2.5 m/day). Offshore wells yielded effective hydraulic conductivities of about 1.1×10^{-3} cm/s (0.9 m/day) to 5.2×10^{-3} cm/s (4.5 m/day). Well transect B demonstrated a higher overall hydraulic conductivity than transect A, despite being separated by only about 30 m alongshore (Table 1).

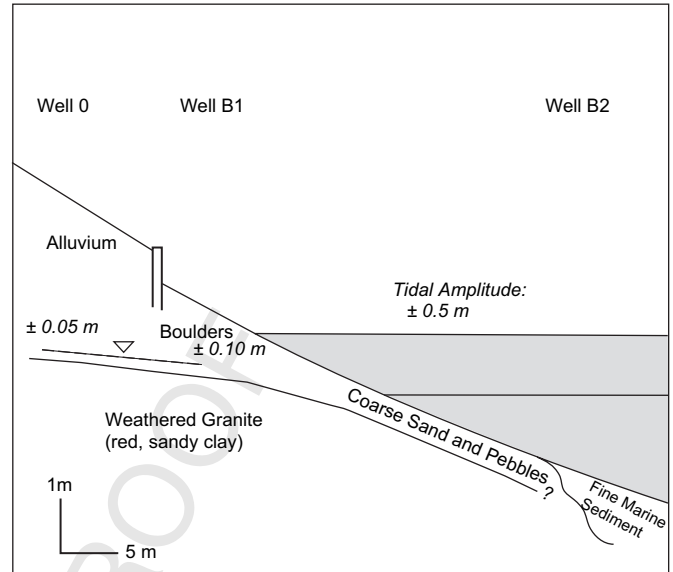


Fig. 4. Conceptual model of geology and hydrogeology at transect B.

3.3. Tidal signal

Relative changes in water levels for Flamengo Bay and well 0 are presented in Fig. 5. The average ($n = 8$, for data of acceptable quality) tidal lag was 14.2 ± 1.5 h and the average ($n = 6$) tidal efficiency was 0.095 ± 0.033 . Assuming an aquifer thickness of 3 m (the saturated weathered bedrock and coluvium) and a specific yield for the aquifer of 0.20, a hydraulic conductivity of 6.1×10^{-3} cm/s (5.3 m/day) was calculated from the tidal lag. The hydraulic conductivity calculated from the tidal efficiency was 5.6×10^{-2} cm/s (49 m/day).

3.4. Darcy's Law estimates of SGD

The hydraulic gradient on land was measured between wells 0 and B1. With a water level change of 0.13 m over a distance of 12.3 m, the hydraulic gradient was calculated to be 0.011, representing a single snapshot of the gradient at that particular moment. This gradient will change at different times in the tidal cycle as the tidal signal is propagated inland. The

Table 1
Hydraulic conductivity (K) values and corresponding fresh SGD

Method	Geologic material	K (m/day)	Fresh SGD (m ³ /day per m shoreline)
Slug/bail test	Weathered bedrock (well 0)	0.09	0.003
Slug/bail test	Beach sand (well 1B)	2.5	0.083
Bail tests	Surf zone granitic sands (wells 2A, 2B)	0.9–2.2	0.03–0.07
Bail tests	Surf zone sands/fine sediments (wells 3A, 3B)	3.3–4.5	0.11–0.15
Tidal signal propagation	Weathered bedrock and beach sand (well 0 to shore)	5.3–49	0.17–1.6

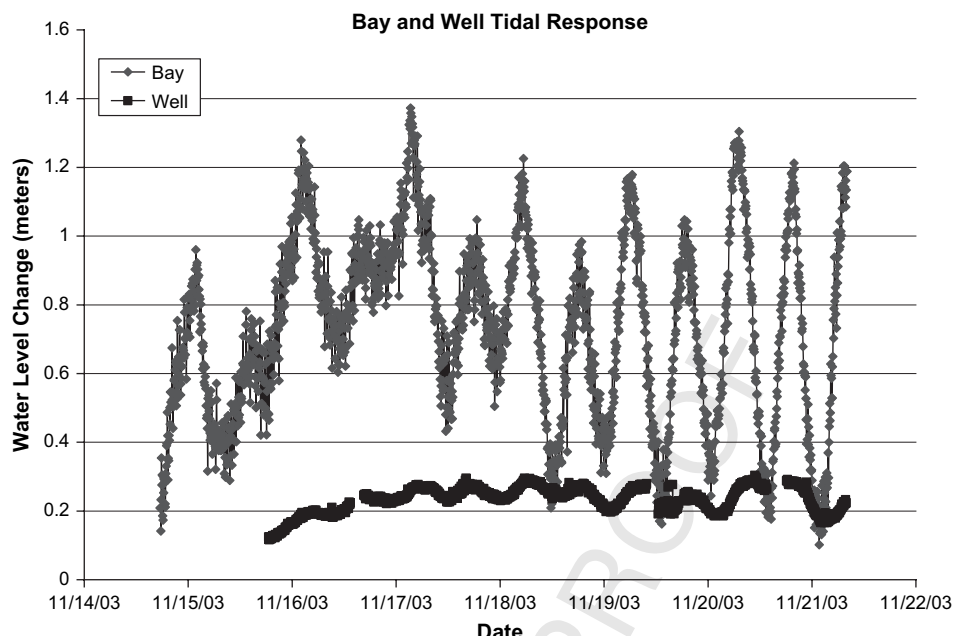


Fig. 5. Tidal signal in Flamengo Bay and well 0.

hydraulic gradient could vary with time by a factor of two from the value given.

It is possible to calculate the discharge of freshwater per unit width of shoreline using Darcy's Law:

$$\frac{Q}{w} = -Kb \frac{dh}{dl}$$

where Q is the discharge (L^3/T), w is the width of shoreline (L), K is hydraulic conductivity (L/T), b is aquifer thickness (L) and dh/dl is the hydraulic gradient.

The aquifer thickness was again taken as approximately 3 m. A range of hydraulic conductivity values has been determined. These values were used to estimate discharge along the shoreline presented in Table 1.

3.5. Water quality

Mini-wellpoints were used at the multiple locations to evaluate groundwater salinity distributions. The salinity was high in the coarse-grained sand and dropped abruptly once the hard, fine-grained layer was penetrated (Fig. 6). Data from the multi-level piezometers revealed a thin fresh water lens present in near-shore sediments about 11 m from the low tide line (Fig. 7). This tongue of freshwater moved within 40 cm of the sediment–water interface at about 8 m offshore (low tide baseline). The freshwater lens was thin and apparently confined by a hard layer to about 1.5 m below the sediments as it moved farther offshore.

Groundwater profiles were also collected for salinity and nutrients at piezometers WH1 and WH2 (Fig. 2). The salinity of the groundwater at WH1 above the coarse–fine sediment transition was approximately 29–30 (Fig. 8a). The groundwater immediately below the transition was in the range of 0–2.

Groundwater at this location appeared to be a net source of nutrients to the overlying water column. In particular, dissolved inorganic nitrogen (DIN) ranged from 5 to 20 μM in the groundwater compared with less than 1 μM in the surface waters (Fig. 8a). Silicate was also highly enriched in the groundwater, ranging from 30 to 120 μM . The piezometer profile at WH2 revealed (Fig. 8b) relatively constant salinity throughout the upper 1.2 m of sediment. DIN was slightly higher on average (up to $\sim 25 \mu\text{M}$) but generally decreased with depth suggesting the sediments were a sink for DIN (e.g., denitrification). Silicate concentrations were similar to the nearshore profile but also decreased with depth. Below 1.2 m depth the piezometer encountered a hard layer which could not be penetrated.

Dissolved oxygen and pH results from the multi-level piezometers are presented in Fig. 9. The dissolved oxygen

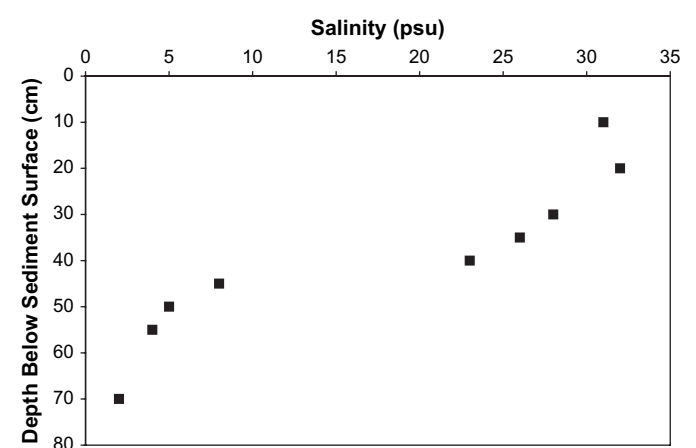


Fig. 6. Porewater salinity profile, located 2 m offshore from the high tide line near Transect B and measured at high tide. The hard, fine-grained layer was encountered around 42 cm, corresponding to the abrupt change in salinity.

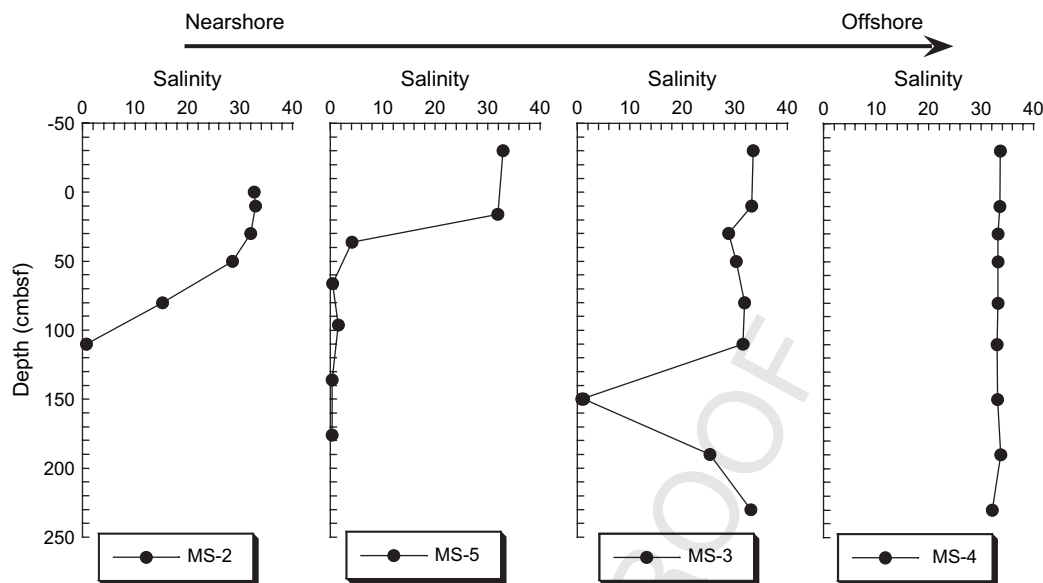


Fig. 7. Pore water salinity versus depth in multi-level piezometer transect extending offshore along transect B, where MS2, MS5, MS3, MS4 correspond to 2.5, 6.5, 10.5, 35 m offshore, respectively. Low saline fluid underlies salt water in upper section of sediment. Tongue of fresh water extends offshore to approximately 10.5 m (MS3) from the low tide line. Freshwater signal has disappeared from pore waters by about 35 m offshore (MS4).

concentrations decrease with depth in the pore water, but are never completely depleted, remaining between approximately 1 and 3 mg/l. Dissolved oxygen was measured in an open sampling cup and the measured oxygen could reflect an artifact of oxygen contamination of the sample. Alternatively, oxygen in the pore waters could reflect the lack of an electron acceptor in these organic-poor sediments. pH values also decrease in the sediment, with the strongest gradients decreasing to a low value of around 5 at the two near-shore sites MS-2 and MS5. The pH profiles mimic the salinity profiles (e.g. Fig. 7) with lower pH occurring in the low salinity water. Na/Cl molar ratio and K/Cl molar ratio versus pH for the same four multi-piezometer stations are presented in Fig. 10. This figure demonstrates that Na/Cl and K/Cl ratios of the low pH and low salinity water differ from seawater values as measured in the overlying water column. In addition, the two ratios differ from each other. The Na/Cl ratio is both elevated and depleted relative to seawater value, while the K/Cl ratio is always lower than seawater value. Assuming that salinity and Cl concentrations are conservative in this system, the variations in pH, K and Na concentrations may reflect mixing between the fresh water end member and seawater, and/or weathering reactions of the granitic rocks and sediments of the region.

4. Discussion

The geology at this site appears to exert a strong control on the distribution and discharge of freshwater. Water flows from the land through the weathered granite beneath the hard layer that separates the overlying coarse-grained sand from the underlying weathered material. This hard layer appears to restrict downward mixing of the saline water while allowing some upward seepage of the freshwater. The

freshwater is again impeded from flowing further offshore where the coarse sand and hard layer end (about 24 m offshore) and the low-permeability, fine-grained, marine sediments begin (Fig. 4).

The calculated freshwater SGDs (Table 1) vary over almost four orders of magnitude. The most reliable estimate of hydraulic conductivity is from the tidal signal propagation data, which averages the permeability over a large volume of aquifer material and provides a more integrated temporal estimate as well. The slug/bail tests provide more of a point measurement and can be sensitive to the well completion and testing methods. It was necessary to assume a specific yield value and aquifer thickness to analyze the tidal data, so uncertainties in those assumptions create uncertainties in the hydraulic conductivity value determined from that method. However, the lower estimate of fresh SGD using the tidal signal approach is similar to values from the bail/slug tests on offshore (surf zone) well sediments, thus, lending credence to the tidal signal approach.

The estimate of freshwater SGD, based on the tidal signal propagation, range over an order of magnitude from 0.17 to 1.6 m³/day per m of shoreline. While the freshwater SGD is probably not evenly distributed across the 24 m of coarse sediment nearest shore, an estimate of the average seepage rate can be made by dividing the SGD by that 24 m distance. The net, upward, freshwater seepage rate thus estimated is 7.1×10^{-3} to 6.7×10^{-2} m/day. This range of rates is at the low end of the range found for SGD from other intercomparison experiments at sites where the geologic materials were more permeable (Burnett et al., 2006). For example, fresh water seepage rates were found to decrease linearly offshore from an estuary on the Atlantic coast of Florida at rates ranging from 0.01 to 1 m/day over a 22 m distance offshore (Martin et al., 2007). The range found in this study is also lower

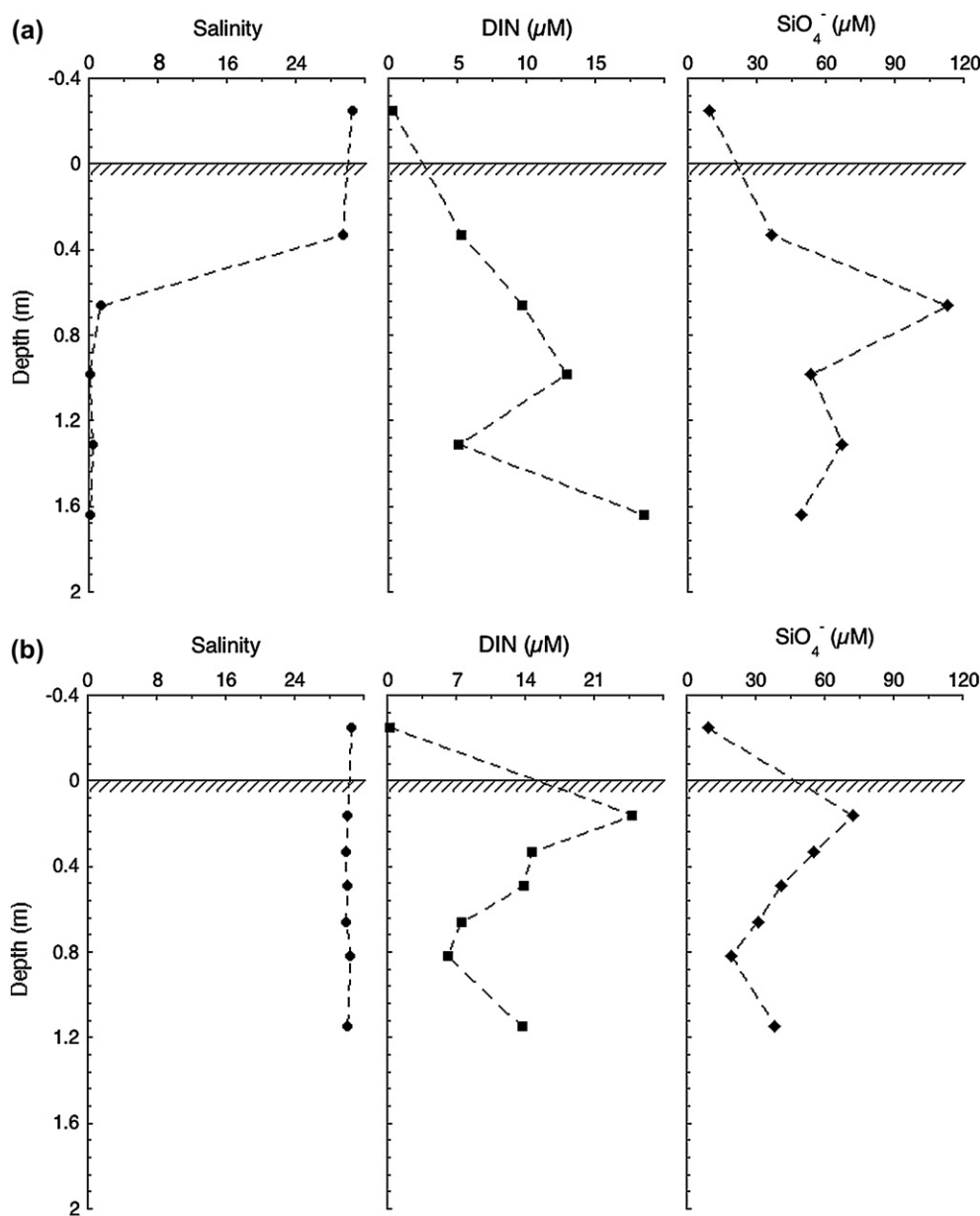


Fig. 8. (a) Nearshore piezometer (WH1) profile of salinity, dissolved inorganic nitrogen, silicate. The hatched line indicates the sediment–water interface; the shaded region is the location of the coarse–fine sediment transition. (b) Offshore piezometer (WH2) profile of salinity, dissolved inorganic nitrogen, silicate. The hatched line indicates the sediment–water interface.

than rates found by seepage meter and geochemical tracer during the Flamengo Bay, Ubatuba intercomparison experiment (Burnett et al., 2006).

Salinity in the pore waters along the multi-level piezometer transect shows freshwater from the surficial aquifer flows seaward. While the lateral offshore extent of freshwater is heterogeneous, it appears that fresh SGD may discharge nearshore primarily within 8 m from shore (using low tide as baseline) (see MSS2 and MS5, Fig. 7). Further offshore along that transect, the freshwater lens is downward-dipping, perhaps confined by a hard clay layer, as suggested from sediment cores collected during the study (Fig. 3). An alternate explanation for the profile in MS5 is that slower upward velocities in the

distal portion of the discharge zone may allow greater exchange across the sediment–water interface. Such exchange has been observed in offshore regions and beach profiles and results from downward diffusion or by mechanisms such as wave and tidal pumping, bioirrigation, or density inversions of salt water overlying fresh water (e.g. Martin et al., 2004, 2007). Coupled to this fresh SGD will be recirculated seawater which enters and exits sediments due to physical (wave, tidal pumping) and biological (bioirrigation) mechanisms (e.g. Martin et al., 2004). This marine pore water exchange will become progressively more important to the total SGD discharge from sediments farther from the shoreline, as evidenced by the salinities in MS3 and MS4.

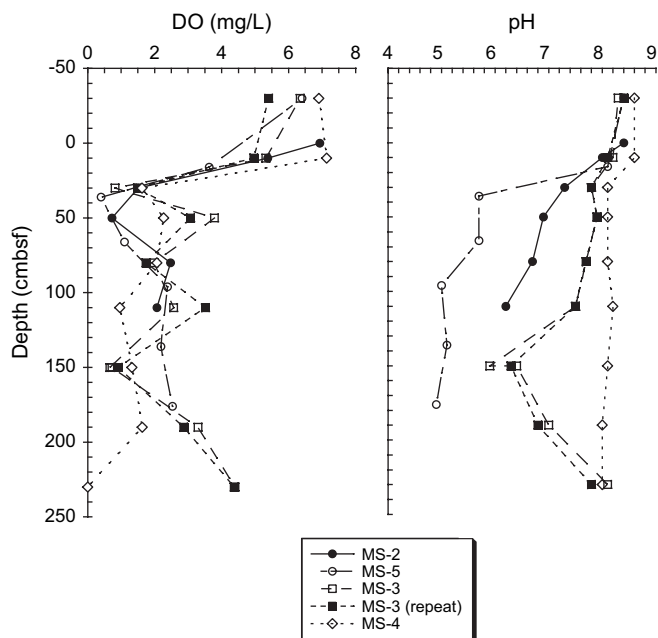


Fig. 9. pH and DO versus depth at the four stations of the multi-level piezometers.

This groundwater seepage rate can be used to estimate the DIN flux to surface waters. If we assume a fresh groundwater DIN endmember of $12 \mu\text{M}$ (12 mmol/m^3), the fresh SGD-derived DIN flux would range between 0.09 and 0.80 mmol N/m^2 per day. These values are nearly an order of magnitude lower than estimates of SGD-derived DIN flux for Chesapeake Bay (Charette and Buesseler, 2004) or South Carolina (Krest et al., 2000), suggesting that subsurface nutrient inputs to this region are minor. However, these estimates do not include the recycled nutrient flux delivered via brackish to saline SGD, hence our DIN flux may be an underestimate of the total SGD-derived flux to this embayment.

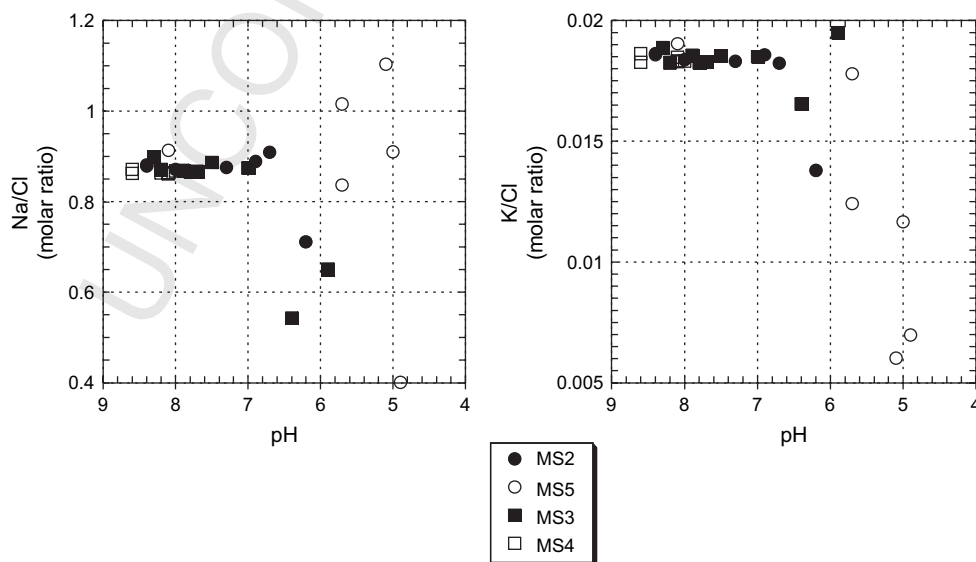
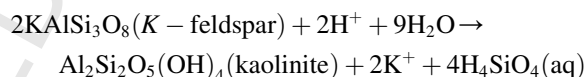
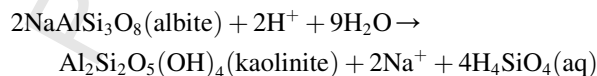


Fig. 10. Na/Cl molar ratio and K/Cl molar ratio versus pH for the four multi-level piezometer stations.

The relatively high dissolved oxygen content (Fig. 9) suggests that there is little regeneration of organic matter in the sediments, which could contribute to the smaller flux of DIN compared with Chesapeake Bay and South Carolina, where sedimentary organic matter is more concentrated. The lowest DO concentrations occur in MS-4 offshore where there is no influence of fresh water discharge. The elevated oxygen concentrations in the other three multisamplers suggest that the fresh groundwater may contain elevated oxygen concentrations, that the oxygen is not reduced during flow through the nearshore sediments, and/or the water resides in the sediment for an insufficient time for the oxygen to be reduced.

If fresh groundwater interacts with the granitic aquifer material during its flow to discharge points at the seepage face, it would be expected that the major element concentrations and pH (Fig. 10) would reflect those alteration reactions. In granitic terrains, water chemistry can change through incongruent dissolution of alkali feldspars to clay minerals such as kaolinite, for example, by the following reactions:



Other weathering products can include the montmorillonite group minerals (e.g. smectite), although kaolinite is typically the phase in equilibrium with natural waters (Huang, 1979). These reactions consume H^+ , which for most terrestrial systems is in the form of carbonic acid (H_2CO_3) resulting from equilibration with atmospheric CO_2 . These reactions also release K^+ , Na^+ , and H_4SiO_4 , which is a weak acid with a dissociation constant of $10^{-9.9}$ at 25°C (Stumm and Morgan, 1996).

Fresh water discharging in the Ubatuba region is characterized by low pH values and K/Cl and Na/Cl ratios that are mostly less than seawater values. These characteristics of the water chemistry indicate that its residence time in the aquifer is insufficient for significant alteration of water chemistry through weathering of feldspar minerals, notwithstanding the observed extensive alteration of the solids in the well boring and cores (e.g. Fig. 3). Weathering of the bedrock may have occurred at an earlier time and is not reflected in the modern water chemistry. Alternatively, the water/rock ratio may be sufficiently high in this high precipitation region that weathering proceeds without significant alteration to the water chemistry. A third possibility is that most of the fresh water flows through unaltered sediments but rapidly mixes with and is lost to the overlying seawater. Restriction of the flow to the unaltered material could result from alteration to clay minerals and the associated reduction in permeability forcing water to flow through less altered zones in the aquifer characterized by higher permeability. Clay mineralogy has not been identified, but presence of montmorillonite, either from in situ weathering or by transportation to the coast, would further reduce permeability as it swells with exchange of Ca to Na interlayer cations. High permeability zones could allow exchange between the shallow permeable sediments and the overlying water column that would produce the elevated salinity found in the upper portions of the multisampler profiles at MS 5 and MS3 (e.g., Martin et al., 2004; Cable and Martin, this issue).

5. Conclusions

The seepage of freshwater is limited at the site by variations in permeability of the sediments overlying the weathered bedrock, with freshwater discharging through the coarse, nearshore sediments but not from the offshore, fine-grained materials. Freshwater seepage rates average on the order of hundredths of meters per day through the approximately 24 m offshore seepage zone. The oxygen concentrations reflect limited organic matter diagenesis, but nonetheless, the SGD appears to contribute DIN to the overlying water column suggesting the nitrogen has a terrestrial source, though the flux is sufficiently low such that other land-derived pathways such as rivers or atmospheric deposition may be as important or greater than SGD. Major element chemical composition of the water appears not to reflect alteration of the granitic aquifer although much of the solid material is altered. The lack of alteration may reflect flow through unaltered sediment which is not observed as low salinity values because of mixing between the overlying seawater and the fresh water in the sediment pore spaces.

Acknowledgments

The Intergovernmental Oceanographic Commission of UNESCO provided travel funds that permitted participation in this field experiment. M.C. and M.A. were also supported by grants from the National Science Foundation (OCE-0095384) and the NOAA-CICEET program (NA17OZ2507-03-723).

References

- Burnett, W.C., Chanton, J., Christoff, J., Kontar, E., Krupa, S., Lambert, M., et al., 2002. Assessing methodologies for measuring groundwater discharge to the ocean. *EOS* 80, 13–15.
- Burnett, W.C., Aggarwal, P.K., Bokuniewicz, H., Cable, J.E., Charette, M.A., Kontar, E., Krupa, S., Kulkarni, K.M., Loveless, A., Moore, W.S., Oberdorfer, J.A., Oliveira, J., Ozyurt, N., Povinec, P., Prvitera, A.M.G., Rajar, R., Ramessur, R.T., Scholten, J., Stieglitz, T., Taniguchi, M., Turner, J.V., 2006. Quantifying submarine groundwater discharge in the coastal zone via multiple methods. *The Science of the Total Environment* 367 (2–3), 498–543.
- Charette, M.A., Buesseler, K.O., 2004. Submarine groundwater discharge of nutrients and copper to an urban subestuary of Chesapeake Bay (Elizabeth River). *Limnology and Oceanography* 49, 376–385.
- Harvey, J.W., Odum, W.E., 1990. The influence of tidal marshes on upland groundwater discharge to estuaries. *Biogeochemistry* 10, 217–236.
- Huang, P.M., 1979. Feldspars, olivines, pyroxenes, and amphiboles. In: Dixon, J.B., Weed, S.B. (Eds.), *Minerals in Soil Environments*, second ed. Soil Science Society of America, Madison, WI, pp. 553–602.
- Hvorslev, M.J., 1951. Time Lag and Soil Permeability in Ground-Water Observations, Bulletin No. 36. *Waterways Exper. Sta. Corps of Engineers*. US Army, Vicksburg, MI, pp. 1–50.
- Jacob, C.E., 1950. Flow of groundwater. In: Rouse, H. (Ed.), *Engineering Hydraulics*. John Wiley Sons, New York.
- Krest, J.M., Moore, W.S., Gardner, L.R., Morris, J.T., 2000. Marsh nutrient export supplied by groundwater discharge: evidence from radium measurements. *Global Biogeochemical Cycles* 14, 167–176.
- Martin, J.B., Hartl, K.M., Corbett, D.R., Swarzenski, P.W., Cable, J.E., 2003. A multilevel pore water sampler for permeable sediments. *Journal of Sedimentary Research* 73, 128–132.
- Martin, J.B., Cable, J.E., Swarzenski, P.W., Lindenberg, M.K., 2004. Mixing of ground and estuary waters: influences on groundwater discharge and contaminant transport. *Ground Water* 42, 1000–1010.
- Martin, J.B., Cable, J.E., Smith, C., Roy, M., Cherrier, J., 2007. Magnitudes of submarine groundwater discharge from marine and terrestrial sources: Indian River Lagoon, Florida. *Water Resources Research* 43, W05440.
- Nuttle, W.K., Harvey, J.W., 1995. Fluxes of water and solute in a coastal wetland sediment, 1. The contribution of regional groundwater discharge. *Journal of Hydrology* 164, 89–107.
- Rebouças, A., 2002. *Águas subterâneas*. In: Rebouças, A., Braga, B., Tundisi, J.G. (Eds.), *Águas Doces no Brasil*, second ed. Escrituras, São Paulo, Brazil.
- Robinson, M.A., 1996. A finite element model of submarine ground water discharge to tidal estuarine waters, PhD dissertation, Virginia Polytechnic Institute, 1996.
- Staver, K.W., Brinsfield, R.B., 1996. Seepage of groundwater nitrate from riparian agroecosystems into the Wye River Estuary. *Estuaries* 19 (28), 359–370.
- Stumm, W., Morgan, J.J., 1996. *Aquatic Chemistry*. John Wiley and Sons Inc., New York, 1022 pp.
- Vanek, V., 1993. Groundwater regime of a tidally influenced coastal pond. *Journal of Hydrology* 151, 317–341.